Unveiling New Magnetic Phases of Undoped and Doped Manganites

Takashi Hotta,[1] Mohammad Moraghebi,[2] Adrian Feiguin,[3] Adriana Moreo,[2] Seiji Yunoki,[4] and Elbio Dagotto[2]

[1]*Advanced Science Research Center, Japan Atomic Energy Research Institute, Tokai, Ibaraki 319-1195, Japan*
[2]*National High Magnetic Field Laboratory, Florida State University, Tallahassee, Florida 32306, USA*
[3]*Department of Physics and Astronomy, University of California at Irvine, Irvine, California 92697, USA*
[4]*International School for Advanced Studies (SISSA), via Beirut 4, 34014 Trieste, Italy*

(Received 2 September 2002; published 17 June 2003)

Novel ground-state spin structures in undoped and lightly doped manganites are investigated based on the orbital-degenerate double-exchange model, via mean-field and numerical techniques. In undoped manganites, a new antiferromagnetic (AFM) state, called the *E*-type phase, is found adjacent in parameter space to the *A*-type AFM phase. Its structure is in agreement with recent experimental results. This insulating *E*-AFM state is also competing with a ferromagnetic metallic phase as well. For doped layered manganites, the phase diagram includes another new AFM phase of the C_xE_{1-x} type. Experimental signatures of the new phases are discussed.

DOI: 10.1103/PhysRevLett.90.247203 PACS numbers: 75.47.Gk, 75.10.–b, 75.30.Kz, 75.50.Ee

In the recent decade, the study of manganites—materials that show a remarkable colossal magnetoresistance (CMR) [1]—has been one of the most important areas of research in condensed matter [2]. This CMR effect occurs when the manganite ground state changes from insulating to ferromagnetic (FM) metallic after a small magnetic field is applied. Based on the concept of two-phase competition [2], the CMR behavior has been successfully qualitatively reproduced in computational simulations employing resistor-network models [3]. However, more work remains to be done to fully understand Mn oxides, both regarding their unusual magneto-transport properties and the nature of the many competing phases.

The appearance of the FM metallic phase in manganites is usually rationalized by the so-called double-exchange (DE) mechanism, based on a strong Hund coupling between mobile e_g electrons and localized t_{2g} spins. On the other hand, the insulating phase in manganites occurs due to the coupling between degenerate e_g electrons and Jahn-Teller (JT) distortions of the MnO_6 octahedra, leading to the various types of charge and/or orbital orders observed experimentally [2].

The parent compound of CMR manganites is undoped $RMnO_3$, where R denotes rare earth ions. For $R =$ La, as is well known, the *A*-type antiferromagnetic (AFM) phase appears with the *C*-type ordering of $(3x^2 - r^2)$ and $(3y^2 - r^2)$ orbitals [4]. By substituting La by alkaline earth ions such as Sr and Ca, holes are effectively doped into the e_g-electron band and due to the DE mechanism, the FM metallic phase appears with its concomitant CMR effect. Most of the discussion in manganites has centered on the many phases induced by doping with holes the *A*-type AFM state, at different values of their bandwidths. In this framework, it is implicitly assumed that the undoped material is always in an *A*-type state. However, quite recently, a new AFM phase has been reported as the ground state in the undoped limit for $R =$ Ho [5,6]. This phase is here called the "*E*-type" spin structure following the standard notation. It is surprising that a new phase can still be found even in the undoped material, previously considered to be well understood. In addition, the nature of the states obtained by lightly doping this *E* phase is totally unknown, and new phenomena may be unveiled experimentally in the near future. Overall, *this opens an exciting new branch of investigations in manganites since novel phases appear to be hidden in the vast parameter space of these compounds.* A clear example has been recently provided by the prediction of a FM charge-ordered (CO) phase at $x = 1/2$ [7,8], which may have been found experimentally already [9].

In this Letter, based on the orbital-degenerate DE model coupled with JT distortions, the ground-state properties of undoped manganites are analyzed by using mean-field (MF) calculations and Monte Carlo (MC) simulations. In our phase diagram at $x = 0$, the *E*-AFM phase is found to exist in a *wide* region of parameter space, adjacent to the *A*-AFM phase in agreement with the experimental results. The *E*-AFM phase is robust when the dimensionality and/or electron-phonon coupling are modified, and its strength is intrinsic of orbital-degenerate DE systems. In the phase diagram and at small electron-phonon coupling the *E*-AFM insulating phase is located next to a FM metallic phase [10]. Light-hole doping x of the *E*-type phase is also discussed and another novel magnetic phase, defined as the "C_xE_{1-x}" phase, is found.

The Hamiltonian studied in this Letter is

$$H = -\sum_{\mathbf{i}\mathbf{a}\gamma\gamma'\sigma} t^{\mathbf{a}}_{\gamma\gamma'} d^{\dagger}_{\mathbf{i}\gamma\sigma} d_{\mathbf{i}+\mathbf{a}\gamma'\sigma} - J_{\mathrm{H}} \sum_{\mathbf{i}} \mathbf{s}_{\mathbf{i}} \cdot \mathbf{S}_{\mathbf{j}} + J_{\mathrm{AF}} \sum_{\langle \mathbf{i},\mathbf{j} \rangle} \mathbf{s}_{\mathbf{i}} \cdot \mathbf{S}_{\mathbf{j}} + \lambda \sum_{\mathbf{i}} (Q_{1\mathbf{i}}\rho_{\mathbf{i}} + Q_{2\mathbf{i}}\tau_{x\mathbf{i}} + Q_{3\mathbf{i}}\tau_{z\mathbf{i}}) + (1/2) \sum_{\mathbf{i}} (\beta Q^2_{1\mathbf{i}} + Q^2_{2\mathbf{i}} + Q^2_{3\mathbf{i}}), \quad (1)$$

where $d_{\mathbf{i}a\sigma}$ ($d_{\mathbf{i}b\sigma}$) annihilates an e_g electron with spin σ in the $d_{x^2-y^2}$ ($d_{3z^2-r^2}$) orbital at site $\mathbf{i}$, and $\mathbf{a}$ is the vector connecting nearest-neighbor (NN) sites. The first term is the NN hopping of e_g electrons with amplitude $t^{\mathbf{a}}_{\gamma\gamma'}$ between γ and γ' orbitals along the $\mathbf{a}$ direction: $t^{\mathbf{x}}_{aa} = -\sqrt{3}t^{\mathbf{x}}_{ab} = -\sqrt{3}t^{\mathbf{x}}_{ba} = 3t^{\mathbf{x}}_{bb} = t$ for $\mathbf{a} = \mathbf{x}$, $t^{\mathbf{y}}_{aa} = \sqrt{3}t^{\mathbf{y}}_{ab} = \sqrt{3}t^{\mathbf{y}}_{ba} = 3t^{\mathbf{y}}_{bb} = t$ for $\mathbf{a} = \mathbf{y}$, and $t^{\mathbf{z}}_{bb} = 4t/3$ with $t^{\mathbf{z}}_{aa} = t^{\mathbf{z}}_{ab} = t^{\mathbf{z}}_{ba} = 0$ for $\mathbf{a} = \mathbf{z}$. Hereafter, t is taken as the energy unit. In the second term, the Hund coupling J_H (> 0) links e_g electrons with spin $\mathbf{s_i} = \sum_{\gamma\alpha\beta} d^\dagger_{\mathbf{i}\gamma\alpha}\boldsymbol{\sigma}_{\alpha\beta}d_{\mathbf{i}\gamma\beta}$ ($\boldsymbol{\sigma}$ = Pauli matrices) with the localized t_{2g} spin $\mathbf{S_i}$ assumed classical with $|\mathbf{S_i}| = 1$. J_H is here considered as very large or infinite. The third term is the AFM coupling J_{AF} between NN t_{2g} spins. The fourth term couples e_g electrons and MnO_6 octahedra distortions, λ is a dimensionless coupling constant, $Q_{1\mathbf{i}}$ is the breathing-mode distortion, $Q_{2\mathbf{i}}$ and $Q_{3\mathbf{i}}$ are, respectively, $(x^2 - y^2)$- and $(3z^2 - r^2)$-type JT-mode distortions, $\rho_{\mathbf{i}} = \sum_{\gamma,\sigma} d^\dagger_{\mathbf{i}\gamma\sigma}d_{\mathbf{i}\gamma\sigma}$, $\tau_{x\mathbf{i}} = \sum_\sigma (d^\dagger_{\mathbf{i}a\sigma}d_{\mathbf{i}b\sigma} + d^\dagger_{\mathbf{i}b\sigma}d_{\mathbf{i}a\sigma})$, and $\tau_{z\mathbf{i}} = \sum_\sigma (d^\dagger_{\mathbf{i}a\sigma}d_{\mathbf{i}a\sigma} - d^\dagger_{\mathbf{i}b\sigma}d_{\mathbf{i}b\sigma})$. The fifth term is the usual quadratic potential for adiabatic distortions and β (≈ 2) is the spring-constants ratio for breathing and JT modes.

In undoped manganites, all oxygens are shared by adjacent MnO_6 octahedra and the distortions are not independent, suggesting that the cooperative effect is even more important than for the doped case $x > 0$. To consider this cooperation, here oxygen ion displacements are directly optimized [11]. Coulomb interactions are indirectly considered by working with a large Hund coupling and with a robust λ, as previously discussed [13].

Let us first describe our two-dimensional (2D) results, since the essential physics behind the stabilization of the E-type phase can be grasped by using MC simulations with relatively short CPU times. The phase diagram on a 4×4 lattice is shown in Fig. 1(a). The continuous curves are obtained by comparing the energies of the competing phases in the MF calculations, while the circles are obtained by monitoring the nature of the dominant spin correlation $S(\mathbf{q})$ in MC simulations. A typical result for $S(\mathbf{q})$ is shown in Fig. 1(b). A new regime characterized by $\mathbf{q} = (\pi/2, \pi/2)$ is clearly observed between the FM and G-AFM phases. The good agreement between MF and MC results in the region of interest shows the high accuracy of the present MF calculations for manganites [14].

In Fig. 1(c), the spin and orbital structure of the novel intermediate phase (E phase) is shown. Along the zigzag chains, t_{2g} spins order ferromagnetically, but they are antiparallel perpendicular to the zigzag direction. In the three-dimensional (3D) case, the MF study shows that the pattern Fig. 1(c) just *stacks* along the z axis, while the spin directions are reversed from plane to plane. Note that the orbital structure is the same as that of the A-AFM phase, namely, the staggered pattern of $(3x^2 - r^2)$- and $(3y^2 - r^2)$-like orbitals. Our investigations show that the

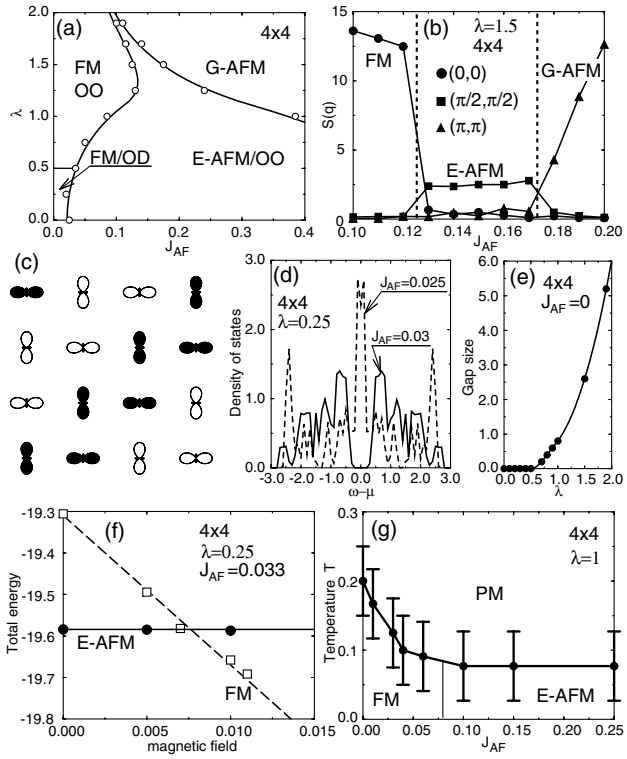

FIG. 1. (a) Phase diagram obtained using the 4×4 lattice. Open circles denote MC results and solid curves are obtained with MF calculations. (b) Spin correlation $S(\mathbf{q})$ vs J_{AF} at $\lambda = 1.5$. (c) Schematic view of the spin and orbital structure of the E-AFM phase. Solid and open symbols denote orbitals with up- and down-spins, respectively. Note the presence of zigzag chains for each spin orientation. (d) Density of states (DOS) obtained by MC simulations at $\lambda = 0.25$. Solid and dashed curves denote, repsectively, the results for E and FM phases. (e) Gap at the Fermi level for the FM phase vs λ. The magnitude is evaluated from the DOS obtained by MC simulations. (f) Total energy vs magnetic field for E-AFM and FM phases. (g) Phase diagram in the (J_{AF}, T) plane at $x = 0$ and $\lambda = 1$, using a 4×4 lattice. Estimations of the Curie and Néel temperatures are evaluated using MC simulations (see text).

E phase is robust at weak and intermediate λ, but for $\lambda > 1.5$, the E-type regime narrows.

A surprising aspect of our results is that the E-type spin arrangement is the ground state for a *wide* range of J_{AF}, even at $\lambda = 0$, indicating that the coupling with JT phonons is *not* a necessary condition for its stabilization. This is in sharp contrast to the case of the A-AFM phase. To understand this point, it is instructive to study the e_g-electronic structure of the zigzag FM chains that appear in the E-phase spin arrangement. Taking J_H as infinity for simplicity, the e_g electrons move only along the zigzag FM chain and cannot hop to the adjacent FM chains. The dispersion energy for e_g electrons in this zigzag FM chain is given by $\varepsilon_k = (2/3)(\cos k \pm \sqrt{\cos^2 k + 3})$ and $(2/3)(-\cos k \pm \sqrt{\cos^2 k + 3})$, indicating that there appears a large *band gap* equal to $4t/3$ at half filling. In fact, even on the 4×4 cluster, there is a clear

gap of the order of t for the E phase in the DOS [Fig. 1(d)]. Since $t^{\mathbf{x}}_{\mu\nu} = -t^{\mathbf{y}}_{\mu\nu}$ for $\mu \neq \nu$, the sign in the hopping amplitude changes periodically in the zigzag situation, leading to a periodic potential for e_g electrons and its concomitant band-insulator nature. In other words, *the E-type phase is stable due to the zigzag geometry of the FM chains that induce a band insulator* [15].

Another related interesting point is the orbital structure of the FM phase. In the strong-coupling region, an orbitally ordered (OO) state appears, essentially with the same pattern as that observed in the E-AFM phase discussed above. All MnO_6 octahedra are distorted at $x = 0$ and the cooperative effect is essential to determine the OO pattern for large λ, irrespective of the spin structure. However, when λ decreases OO disappears and an orbital disordered (OD) new phase is observed. This is a metallic phase according to the DOS in Fig. 1(d). The OO-OD transition is monitored by the gap size at the Fermi level in the DOS [Fig. 1(e)]. The transition observed using a 4×4 cluster is robust, although the actual critical value may change in larger systems [16]. Note that in the small λ region, interorbital same-site Coulomb repulsion may be important and, as a consequence, the stability of the FM metallic phase found here needs further confirmation.

Assuming the FM metallic phase survives the inclusion of Coulomb interaction, interesting effects can be predicted. Note that the OD-FM phase is next to the insulating E-AFM phase for $\lambda \lesssim 0.5$ (the E phase is insulating with a DOS gap both at small and large λ). Since the competition between FM metallic and insulating phases is at the heart of the CMR phenomena, by tuning experimentally the lattice parameters in $RMnO_3$ it may be possible to observe the magnetic-field induced metal-insulator transition even in undoped manganites. In fact, small magnetic fields of a few teslas indeed induce a phase transition between E and FM phases [see Fig. 1(f)], with a concomitant jump in the magnetization. This interesting speculation deserves further work.

Let us discuss the effect of thermal fluctuations. For this purpose, both T_C (Curie temperature) and T_N (Néel temperature) are estimated from MC simulations in 4×4 clusters [17] [Fig. 1(g)]. Our estimated T_C is found to decrease with increasing J_{AF}, and in the E-AFM phase, T_N becomes almost constant. The E phase can be disordered by thermal fluctuations faster upon heating than the FM phase. Provided that our estimated T_C in the 2D system is related to T_N with the A-AFM phase of 3D lattices, Fig. 1(g) mimics well the experimental results for the changes of T_N by R-ion substitution in $RMnO_3$ [6].

Now let us turn our attention to the effect of dimensionality. In Fig. 2(a), using bilayer $4 \times 4 \times 2$ clusters, the ground-state energy per site is depicted vs J_{AF} at $\lambda = 1.5$ both for numerical optimization [18] and MF calculations, with a good agreement between them. Figure 2(b) is the phase diagram on a $4 \times 4 \times 4$ cubic lattice, obtained only by the MF approximation, since MC calculations in this case are too CPU time-consuming (previous MF-MC comparisons suggest that this MF phase diagram is accurate). In the strong-coupling region, there occurs a chain of transitions from FM $\rightarrow$ A-AFM $\rightarrow$ C-AFM $\rightarrow$ G-AFM phases [19], already obtained in $2 \times 2 \times 2$ calculations [4]. The present result shows that size effects are small in undoped strongly coupled manganites, which is intuitively reasonable. Note that near $\lambda \sim 1.6$, the A-AFM phase is adjacent to the E-type state. This region could correspond to the actual situation observed in experiments for $RMnO_3$: When the ionic radius of the R site decreases, T_N of the A-AFM phase decreases as well, and eventually the E-AFM phase is stabilized for $R =$ Ho [6]. In the weak-coupling region, the E-type phase is stable in a wide range of J_{AF}, as in 2D.

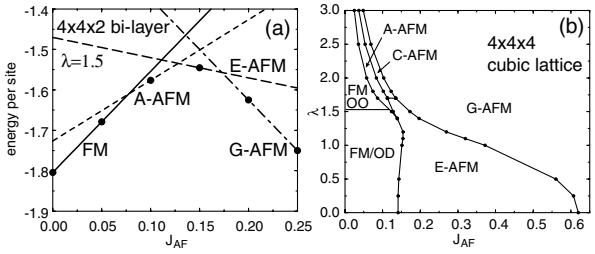

FIG. 2. (a) Energies of the FM, A-AFM, E-AFM, C-AFM, and G-AFM phases on $4 \times 4 \times 2$ bilayer lattices ($\lambda = 1.5$). Solid circles indicate the results of optimizations, while lines denote the MF results. (b) Phase diagram for the $4 \times 4 \times 4$ cubic lattice. All solid lines emerge from MF calculations.

Consider now the very interesting effect of light-hole doping on the E phase. Hole doping is studied in the weak-coupling limit, since the E-type phase is well understood at $\lambda = 0$. Figure 3(a) shows the ground-state phase diagram in the (x, J_{AF}) plane, obtained using analytic calculations on 2D lattices at $\lambda = 0$. A remarkable feature of this phase diagram is the appearance of the novel C_xE_{1-x} phase, composed of long-period zigzag FM chains, antiferromagnetically coupled to each other [see Fig. 3(b) for $x = 1/6$]. As the doping fraction grows, the previously reported states at intermediate and high doping will eventually be reached [8,12]

From the doping dependence of the energies for FM and C_xE_{1-x} phases (not shown), it is concluded that phase separation occurs between those two phases for $0 \lesssim x \lesssim 0.5$. The C_xE_{1-x} is itself a microscopic phase-separated state, since the C- and E-type structures are mixed at the lattice-constant length scale. This phase is expected to be made unstable easily near the phase boundary region, and to turn into a phase-separated state with a mixture of metallic FM and insulating C_xE_{1-x} clusters, which may induce CMR effects.

In the C_xE_{1-x} phase, e_g holes tend to localize in the C-type region [hatched squares in Fig. 3(b)], i.e., in the straight segment portion of the zigzag FM chain, and as a consequence charge ordering of the "stripe" form [20] is induced even at $\lambda = 0$ [21]. This causes incommensurate

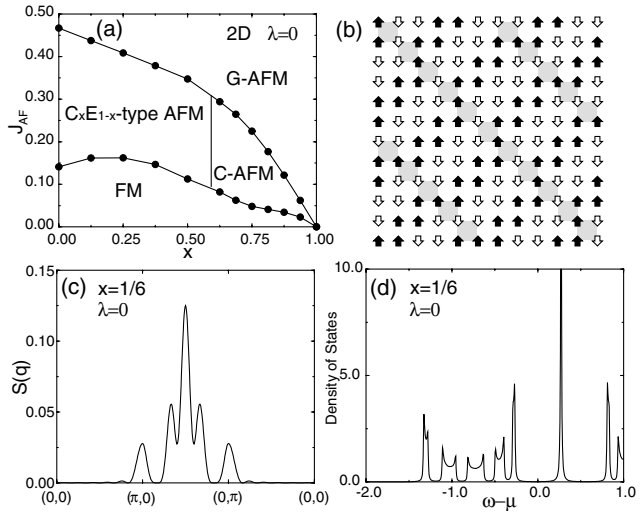

FIG. 3. (a) Phase diagram in the (x, J_{AF}) plane for layered manganites at $\lambda = 0$ obtained by analytic calculations. (b) Schematic view for spin structure of the C_xE_{1-x}-type phase at $x = 1/6$. Hatched squares denote hole-rich C-type regions. (c) $S(\mathbf{q})$ and (d) the DOS in the $C_{1/6}E_{5/6}$-type phase.

peaks in the charge correlation at $\mathbf{q} = (2\pi x, 2\pi x)$. The spin sector is also nontrivial [Fig. 3(c)] and the state is an insulator [see Fig. 3(d)] [22].

In summary, the extended phase diagrams of manganites for $x = 0$ and $x > 0$ have been discussed. A novel E-AFM phase, stabilized at $x = 0$ in the region of weak and intermediate couplings, is adjacent to both FM metallic and A-AFM states. Several features of the E- to A-AFM transition, at least qualitatively, agree with currently available experimental results. For $x > 0$, a microscopically inhomogeneous C_xE_{1-x}-AFM state is predicted. This state may contribute to the phase separation tendencies widely observed experimentally for $0 \lesssim x \lesssim 0.5$ [2,3,23]. The discovery of these many "hidden" interesting phases in real manganites—undoped and doped—should be actively pursued experimentally. This will open a new subbranch of investigations in the already much interesting context of Mn oxides.

The authors thank T. Kimura and K. Ueda for discussions. T. H. is supported by a Grant-in-Aid for Scientific Research from the Ministry of Education, Culture, Sports, Science, and Technology of Japan. E. D. and A. M. are supported by the NSF Grant No. DMR-0122523.

[1] See, for instance, *Colossal Magnetoresistance Oxides*, edited by Y. Tokura (Gordon & Breach, New York, 2000).
[2] E. Dagotto *et al.*, Phys. Rep. **344**, 1 (2001); see also E. Dagotto, *Nanoscale Phase Separation and Colossal Magnetoresistance* (Springer-Verlag, Berlin, 2002).
[3] M. Mayr *et al.*, Phys. Rev. Lett. **86**, 135 (2001); J. Burgy *et al.*, Phys. Rev. Lett. **87**, 277202 (2001).
[4] T. Mizokawa and A. Fujimori, Phys. Rev. B **54**, 5368 (1996); W. Koshibae *et al.*, J. Phys. Soc. Jpn. **66**, 957 (1997); S. Ishihara *et al.*, Phys. Rev. B **55**, 8280 (1997); R. Maezono *et al.*, Phys. Rev. B **57**, R13 993 (1998); L. F. Feiner and A. M. Oleś, Phys. Rev. B **59**, 3295 (1999); P. Horsch *et al.*, Phys. Rev. B **59**, 6217 (1999); J. van den Brink *et al.*, Phys. Rev. B **59**, 6795 (1999); T. Hotta *et al.*, Phys. Rev. B **60**, R15009 (1999); M. Capone *et al.*, Eur. Phys. J. B **17**, 103 (2000).
[5] A. Muñoz *et al.*, Inorg. Chem. **40**, 1020 (2001).
[6] T. Kimura *et al.*, cond-mat/0211568.
[7] S. Yunoki *et al.*, Phys. Rev. Lett. **84**, 3714 (2000).
[8] T. Hotta *et al.*, Phys. Rev. Lett. **84**, 2477 (2000).
[9] J. Loudon *et al.*, Nature (London) **420**, 797 (2002).
[10] Although $x = 0$ corresponds to one e_g electron per site which naively may suggest insulating behavior, there are two active orbitals and the mean density per state is 1/2.
[11] In practice, considering sites **i** and **i** + **a**, the oxygen in between is allowed to move along the **a** axis; i.e., buckling and rotations are neglected. In the 2D case apical oxygens are assumed to be fixed [12].
[12] T. Hotta *et al.*, Phys. Rev. Lett. **86**, 4922 (2001).
[13] Since JT distortions suppress double occupancy, as on-site Coulomb interaction does, a robust λ mimics the effect of interorbital Coulomb repulsion. In addition, a large Hund coupling emulates a large same-orbital Hubbard U term [2] (see Ref. [14]).
[14] T. Hotta *et al.*, Phys. Rev. B **62**, 9432 (2000).
[15] A similar mechanism has been discussed by some of the authors for the CE-type phase at $x = 0.5$ [8].
[16] The metal-insulator transition driven by JT phonons occurs at a *finite* value of λ in the infinite lattice [T. Hotta, Phys. Rev. B **67**, 104428 (2003)].
[17] While finite clusters do not show true thermodynamic singularities, a rapid increase in the strength of correlations is observed at fairly well defined temperatures, here referred to as T_{N} and T_{C} for simplicity [2].
[18] Both spin directions and oxygen positions are optimized.
[19] Note that the FM-OO state of Fig. 2(b) is another phase not previously observed experimentally, here predicted to exist for low-J_{AF} manganites at $x = 0$.
[20] Stripes in manganites establish an interesting analogy with similar physics in cuprates and nickelates [see J. M. Tranquada *et al.*, Nature (London) **375**, 561 (1995)].
[21] Further work is needed to check the stability of the structure against long-range Coulomb interactions.
[22] For $x > 0.5$ and large λ, the C_xE_{1-x} phase is compatible with the so-called Wigner-crystal CO-OO structure suggested for $x = 2/3$ and $3/4$ in $La_{1-x}Ca_xMnO_3$ [P. G. Radaelli *et al.*, Phys. Rev. B **59**, 14440 (1999); M. T. Fernández-Díaz *et al.*, Phys. Rev. B **59**, 1277 (1999)]. However, the bistripe CO-OO phase suggested by Mori *et al.* [S. Mori *et al.*, Nature (London) **392**, 473 (1998)] is consistent with the $C_{1-x}E_x$-AFM state, emerging from the competition with the Wigner-crystal structure [8]. Experimentally, the C_xE_{1-x}-AFM phase has been reported for $x > 0.5$ in $Nd_{1-x}Sr_{1+x}MnO_4$ [T. Kimura *et al.*, Phys. Rev. B **65**, 020407(R) (2001)].
[23] D. Arovas and F. Guinea, Phys. Rev. B **58**, 9150 (1998); G. R. Blake *et al.*, Phys. Rev. B **66**, 144412 (2002).